Journal of Loss Prevention in the Process Industries 80 (2022) 104862

Contents lists available at ScienceDirect

Journal of Loss Prevention in the Process Industries

journal homepage: www.elsevier.com/locate/jlp

Determination of the explosion parameters of methane-air mixtures as function of the ignition source and the volume and shape of the explosion chambers

Martina-Inmaculada Álvarez-Fernández [a,*], María-Belén Prendes-Gero [b], Isaac Pola-Alonso [c], Lucía Conde-Fernández [a], Juan-Carlos Luengo-García [d]

[a] Department of Mining Exploitation and Prospecting, School of Mining, Energy and Materials Engineering of Oviedo, University of Oviedo, Oviedo, Asturias, Spain
[b] Department of Construction and Manufacturing Engineering, Polytechnic School of Engineering of Gijón, University of Oviedo, Gijón, Asturias, Spain
[c] Institute for Economic Development of the Principality of Asturias, Government of the Principality of Asturias, Asturias, Spain
[d] Department of Energy, School of Mining, Energy and Materials Engineering of Oviedo, University of Oviedo, Oviedo, Asturias, Spain

ARTICLE INFO

Keywords:
Methane
Air mixtures
Explosion characteristics
Experimental study
Maximum pressure characteristics
Pressure gradients
Pressure acceleration

ABSTRACT

The combination of methane - air can cause potentially explosive mixtures, which in contact with an energy source can ignite, resulting not only in the destruction of infrastructure but also in the death of people. The aim of this paper is to study the ignition of methane - air mixtures with different concentration of methane, as a function of the ignition sources used and the volume and geometry of the explosion chamber. For this purpose, the 'Dynamic Behaviour of the Rock mass (DinRock)' research group of the University of Oviedo has designed and manufactured 3 explosion chambers of different sizes and shapes, instrumented with dynamic pressure sensors and accelerometers. In addition, the ignition process has been recorded with a high-speed camera. With the results obtained after a laboratory-scale experimental campaign, the maximum pressure reached, the pressure gradients and the acceleration of the pressure waves were analysed. Thus, it has been determined that the maximum pressure reached is independent of the ignition source used and the chamber volume, but not of the chamber geometry. Methane (CH_4) concentrations between 8.0 and 9.0% generated the highest pressures between 1.5 and 2.5 MPa. A correlation between peak acceleration and peak pressure has also been established allowing to identify whether a deflagration or a detonation has occurred.

1. Introduction

The combination of methane - air can cause potentially explosive mixtures, which in contact with an energy source can ignite, resulting not only in the destruction of infrastructure but also in the death of people. Examples of this are the accidents in the underground coal mines of Mount Kembla (Australia) (Radford, 2014) and Benxihu Colliery (China) (Dhillon, 2010) or the gas explosion of an underground pipeline in Kaohsinung (Taiwan) (Yang et al., 2016).

The severity of these explosions depends on several factors (Mynarz et al., 2012) (Xu et al., 2020). These include the explosion range or concentration of methane that can ignite the mixture (Kundu et al., 2016), the ventilation conditions of the spaces where the explosion occurs and which we will call chambers (Solberg et al., 1981), the obstacles in these chambers that affect the flame acceleration process (Johansen and Ciccarelli, 2009) and the location of the ignition points (Kindracki et al., 2007) (Rocourt et al., 2014).

Multiple studies place the limits of the explosion range between 5 and 15% methane concentration (Kundu et al., 2016). Thus, when the methane concentration is below the lower explosive limit, the amount of methane is so low that ignition cannot occur, while if the concentration is above the upper explosive limit, the low amount of oxygen prevents ignition (Gharagheizi, 2008).

The effects of chambers, their shapes, and their ventilation are other factors that have been extensively analysed (Ajrash et al., 2016a). studied the impact of chamber geometry and ignition energy on the pressure reached in the explosion and the flame propagation velocity (Ma et al., 2018). examined for a spherical chamber with horizontal piping the effects that different ignition positions have on pressure and flame transmission (Li et al., 2020). analysed the effect that a

* Corresponding author.
E-mail address: inma@uniovi.es (M.-I. Álvarez-Fernández).

https://doi.org/10.1016/j.jlp.2022.104862
Received 28 April 2022; Received in revised form 20 July 2022; Accepted 23 August 2022
Available online 31 August 2022

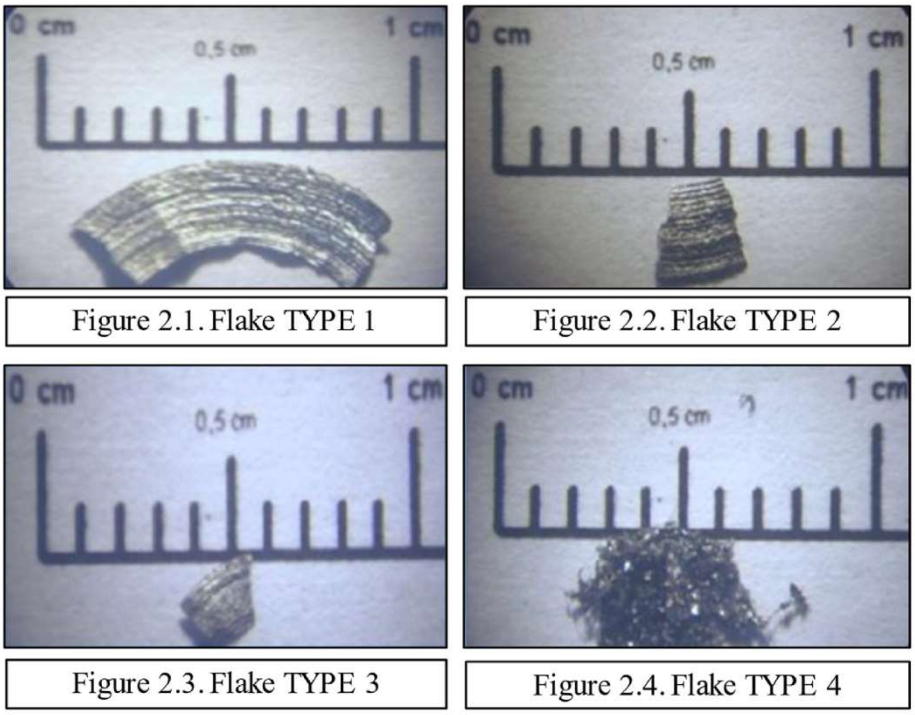

Fig. 1. Photographs of flakes used in the tests.

top-ventilated chamber has on methane concentration and ignition position (Li et al., 2019). studied a vented explosion in a manhole and found a relationship between methane concentration and ignition point position (Li et al., 2020). evaluated how the natural/forced overhead ventilation of a chamber affects the methane concentration and the position of the ignition point for an explosion to occur.

The effects of the initial ignition source on the explosion and flame properties were investigated using laboratory and large scale explosion chambers (Cashdollar, 1996), (Cashdollar, 2000). Other authors focused their research on the ignitors (Ajrash et al., 2016b). analysed the relation between the concentration of methane and the sensitivity of the ignitors while (Going et al., 2000) studied the influence of the ignitors energy effects on the flammability limit of a coal dust.

Research to date has advanced our understanding of explosions resulting from methane-air mixtures. However, accidents are still occurring all over the world, being notorious the high incidence of explosions of this type in developed countries such as the United States or Australia, in spite of their strong safety and control measures.

In this paper, the ignition of explosive methane atmospheres is analysed as a function of parameters such as the methane content in the explosive atmosphere, the volume of the chamber where the explosion occurs and its geometry. To this end, tests are carried out at different scales that reproduce a methane explosion with different ignition sources, analysing the maximum pressure of each explosion, the pressure gradient and the acceleration of the shock waves.

2. Methodology

Laboratory tests have been carried out on different equipment, at several scales, designed and manufactured by the Research Group 'Dynamic Behaviour of the Rock mass (DinRock)' of the University of Oviedo. Different parameters have been analysed: ignition sources, methane concentrations, geometries and sizes of the explosion chambers.

Table 1
Characteristics of the laser used in the tests.

- Wire ignition increasing the temperature of a metal wire by means of electrical energy (Joule dissipation). The objective is analyse the behaviour of the mixture methane-air once the ignition is reached. In this case, two types of wires are examined: a steel wire with a melting temperature of 1535 °C and a nichrome wire with a melting temperature of 1400 °C (Fig. 2). The current is applied by means of an adjustable current source at 12 V and 8 A. This source is connected to a 220 to 12 V power transformer. The power is supplied by a plug connected to the mains, which is routed to the regulator and the current transformer, and from there to the ignition wire. After testing various lengths of steel wire, it was concluded that 120 mm length and 0.4 mm diameter of steel wire were the most suitable dimensions for the execution of the explosions. With the two types of wires, the temperature reached, once the electric current is applied, is measured using a Keller pyrometer with a temperature range of 600 to 2,500 °C.

Characteristics	Value
Mean Power	50 W
Peak Pulse Power	6000 W
Pulse energy	80 J
Pulse length	0.5–50 ms
Spot Size	0.3–2 mm

2.1. Ignition sources

Explosions are generated at a specific point and propagate through the surrounding gas. Two different types of ignition sources with different objectives are used:

- Laser-induced ignition applying pulses of energy (Phuoc and White, 1999), (Beduneau et al., 2003) to steel flakes obtained from mining

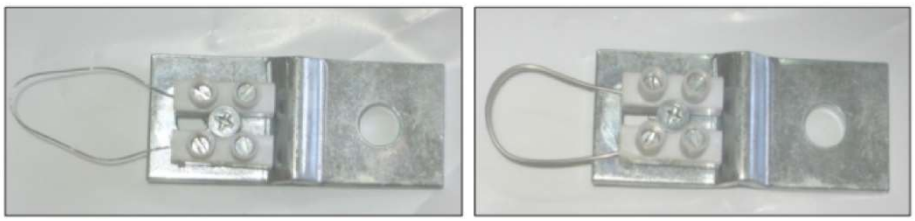

Fig. 2. Steel wire, left, and nichrome wire, right.

Fig. 3. Chamber 1, on the left. Chamber 2, on the right.

Fig. 4. Chamber 3.

tools (Taveau et al., 2019). The goal is to analyse the influence of the size of the flake in the explosion and the minimum energy required for its ignition. For that, four sizes of flakes are analysed type 1, 2, 3 and 4 (Fig. 1).

The laser combustion was initiated with a Rofin Sweet Spot, manufactured by Rofin-Baasel Lasertech GmbH & Co. KG, a 1064 nm neodymium-yttrium-garnet laser with the characteristics shown in Table 1.

2.2. Explosion chambers

To analyse the geometry and size, three explosion chambers of different shapes and dimensions, sealed and prepared to withstand high pressures, were designed.

The quasi-spherical Chamber 1 (Fig. 3) has an internal volume of 6.1 dm^3. It is made of 8.0 mm thick steel and has dimensions of 24.5 cm height and 28.0 cm maximum diameter. It is equipped with 8 sleeves to attach the necessary instrumentation to monitor the tests and a safety glass in the upper part. This glass allows the visualisation and video recording of the tests, and the ignition with both laser and steel cable where the measurements are taken with a pyrometer. For the selection of the glass, the behaviour of square and round crystals of 12.0, 18.0 and 20.0 mm thicknesses subjected to inert gases at high pressure is analysed, but the square crystals have an accumulation of pressures in the corners which can cause them to break (Rivas, 2016). Finally, the chamber is designed with a 12.0 mm thick, bullet-resistant, rounded laminated glass of 135.0 mm diameter.

Chamber 2 has a very similar shape to the first chamber as shown in Fig. 3, but with an interior volume of 38.0 dm^3.

Chamber 3 (Fig. 4) has a tubular geometry 118.0 cm long, with a maximum internal diameter of 20.3 cm and an inner volume of 38.7

Table 2
Technical characteristics of the EPXH-P3 35 and 70 bar pressure sensors.

Technical characteristics	Sensor 1	Sensor 2
Measurement range	7.00 MPa	3.50 MPa
Maximum burst pressure	14.00 MPa	7.00 MPa
Resonant frequency	200 kHz	150 kHz
Thermal sensitivity shift	±1.5 full scale	±1.5 full scale
Excitation	10 V DC	10 V DC
Impedance in	1200 Ω	1200 Ω
Impedance out	350 Ω	350 Ω
Maximum operating temperature	1650 °C	1650 °C
Zero offset	±10 mV typical	±10 mV typical
Type of pressure measurement	Relative	Relative

Table 3
Technical characteristics of the triaxial accelerometer KS813B.

Technical characteristics	Value
Acceleration range	±55 g
Measurement in axes	X, Y, Z
Destruction limit	4000 g
Constant current supply	2–20 mA
Output type	IEPE
Resonant frequency	15 kHz
Output impedance	<250 Ω
Transverse sensitivity	<5%
Operating temperature range	−20 to 90 °C
Protection's degree	IP67
Weight without cable	115 g

Table 4
Characteristics of the digital mass flowmeter used in the tests.

Technical characteristics	Value
Accuracy	±0.8% measurement reading ±0.2% full scale
Flow range	From 0.01 to 0.5 g/s based on CO_2
Maximum operating pressure	<6.4 MPa
Input pressure	<2.0 MPa
Output pressure	<1.5 MPa
Operating temperature	−10° a 70 °C

dm^3. Its shape makes it possible to simulate, on a small scale, the propagation of an explosion in a gallery or tunnel. It is equipped with two safety glasses and intermediate areas for the attachment of sensors.

2.2.1. Instrumentation

Pressure sensors of type EPXH-P3 are attached to all chambers, allowing 50,000 data per second and with measuring ranges of up to 3.50 and 7.00 MPa (Table 2).

In addition, triaxial accelerometers KS813B are attached which measure the vibration accelerations occurring in the chambers in all three directions (Table 3).

Finally, recordings of the ignition and explosion are made using a Kodak SR500 high-speed camera, which can record 500 images per second.

2.3. Methane concentration

A very important factor in the analysis of methane-air explosions is the concentration of methane that is introduced into the chambers to generate an explosive mixture. To measure and control the gas flow, a digital thermal mass flow meter from Bronkhorst Hi-Tech is used. Its characteristics are given in Table 4.

The flow meter is controlled by the FlowDDE software, which is provided by the manufacturer of this equipment. At the end of the flow meter that connects this equipment with the gas tank, a shut-off valve is installed to prevent the undesired flow of gas. In addition, a filter is also added to prevent the entry of particles into the flowmeter. At the opposite end, which connects the flowmeter to the explosion chamber, a non-return valve is provided to prevent gas flow in the wrong direction.

Table 5
Methane concentration as a function of air's humidity.

Humidity (%)	m_{CH4}	Moles Total Mixture (m_{TM})	Methane concentration = m_{CH4}/m_{MT} (%)
0.0	1.0	1.0 + 2.0 · (1.0 + 3.8) = 10.5	9.5
0.5	1.0	1.0 + 2.0 · (1.0 + 3.8) + 0.5 = 11.0	9.1
1.0	1.0	1.0 + 2.0 · (1.0 + 3.8) + 1.0 = 11.5	8.7
2.0	1.0	1.0 + 2.0 · (1.0 + 3.8) + 2.0 = 12.5	8.0

Table 6
Summary of tests carried out and explosions obtained.

	Explosions	Trials	Total tests
Chamber 1			
Laser	95	56	151
Steel wire	30	59	89
Chamber 2			
Steel wire	10	2	12
Chamber 3			
Steel wire	21	14	35
Total	156	131	287

All tests are carried out with methane-air mixtures whose combustion reaction is given, for dry air and without the presence of other gases, by Expression (1)

$$CH_4 + 2\left(O_2 + \frac{79}{21}N_2\right) = CO_2 + 2H_2O + 2\left(\frac{79}{21}N_2\right) \quad (1)$$

However, the tests are performed by introducing atmospheric air, therefore, humidity is also incorporated, so the combustion expression is transformed into Expression (2).

$$CH_4 + 2\left(O_2 + \frac{79}{21}N_2\right) + X_gH_2O = CO_2 + 2H_2O + 2\left(\frac{79}{21}N_2\right) + X_gH_2O \quad (2)$$

Therefore, when calculating the methane concentration in the total combustion mixture, considering Expression (2), it is observed that it varies for different humidity contents (Table 5). Table 5 shows that with dry air and under ideal conditions, the methane concentration is 9.5%. However, an increase in air humidity causes a decrease of this value. In other words, combustion is carried out with lower concentrations of fuel, also reducing the temperature and pressure reached during combustion.

3. Results and discussion

The tests are carried out under room conditions (19 °C and atmospheric pressure) with different methane-air mixtures, in which the methane concentrations have been varied. The analysis parameters are: the critical ignition energy or minimum energy to start the combustion of the flammable mixture when the laser is employed as ignition source; the explosion range or methane concentration that can ignite the sample; the maximum pressure reached in the explosions; the rate of pressure or variation of the pressure increase as a function of time; and the vibrations produced in the chambers. In total, 287 tests were performed, 156 of which included an explosion, while the rest were preparation tests, mixtures in which combustion did not propagate or anomalous results. Table 6 presents a summary of the tests performed.

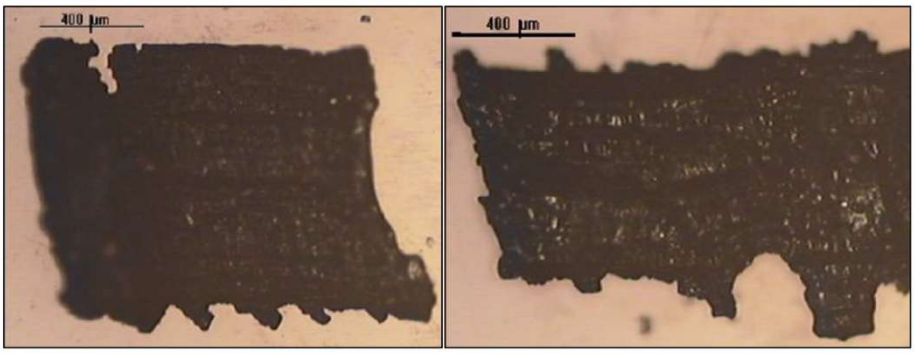

Fig. 5. Real flakes detached during the friction of a tool against a rock (seen under the microscope).

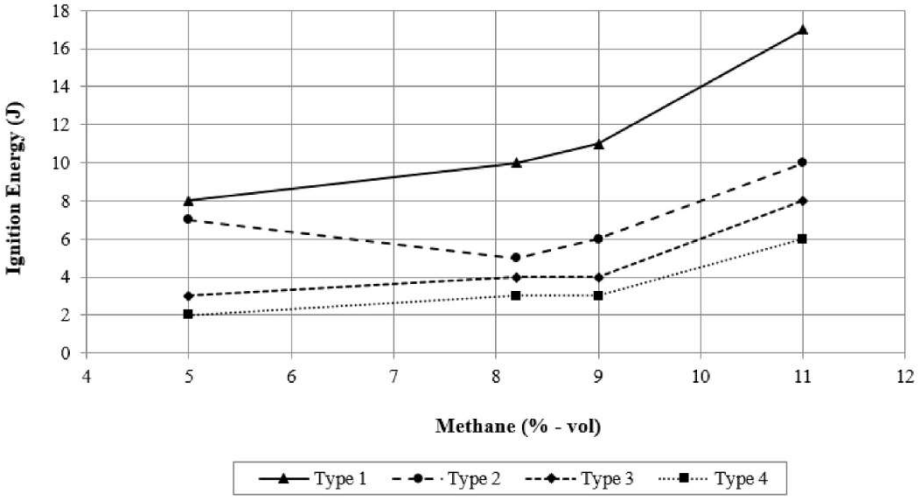

Fig. 6. Energies applied to flakes to obtain ignition.

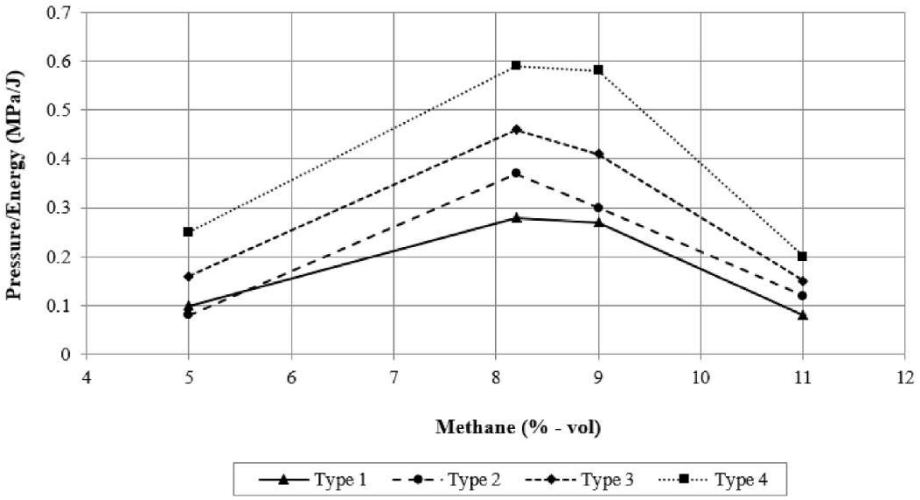

Fig. 7. Pressure - energy ration as a function of flake size.

3.1. Ignition energy

The minimum energy required for ignition to occur is analysed as a function of methane content and flake size, with sizes 2 and 3 being similar to the sizes of flakes released during the friction of a tool against rock (Fig. 5).

For the calculation of the energy required, ignition is realised with a laser. From Fig. 6, it can be seen that the larger the flake size, the more energy must be applied to the flake to initiate ignition, up to 17 J for Type 1 flakes (size around 1 cm) and a methane concentration of 11.0%.

Considering that the laser diameter is constant and equal to 0.3 mm, this increase in critical energy with the size of the flake is due to the fact that larger flakes have a larger volume to distribute the laser energy. Therefore, the temperature reached, for the same energy, is lower and

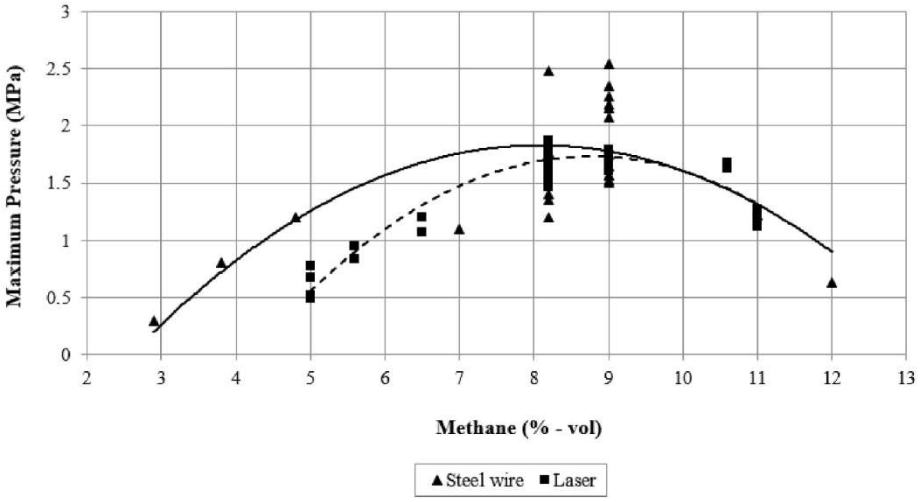

Fig. 8. Maximum pressure reached in wire and laser ignition in Chamber 1.

prevents ignition from occurring.

In contrast to the critical energy, the size of the flake has little influence on the maximum pressure reached in the explosion. However, taking into account that small flakes need less energy to reach the same pressures, it can be said that they are the most energy efficient and therefore the most dangerous, as shown in Fig. 7. From Fig. 7 it can be seen that the maximum explosion pressure per unit of energy input is highest for flakes of type 4 and methane concentrations between 8 and 9.0%. This is lower than the concentration calculated for an ideal combination of dry air - methane and no other gases.

3.2. Maximum explosion pressure

A total of 240 tests were carried out in Chamber 1. Of these, 95 were ignited by laser ignition, while another 30 were ignited using steel wire as the ignition source. For these tests, Type 2 and 3 flakes were used, which are similar in size to real flakes released during the collision of a mechanical tool with a rock.

Fig. 8 shows the maximum pressure versus methane concentration used in each test. It shows that, when steel wire is used as the ignition method, explosions are achieved at methane concentrations of only 2.9%, well below the lower explosive limit of 5.0% reported in most studies (Kundu et al., 2016), which is also the limit at which the first explosions occur when lasers are used as igniters. Furthermore, only one of the seven tests with 12.0% methane achieves ignition when using the steel wire as a source, while the maximum concentration of methane at which ignition is achieved when using the laser as a source is 11.0%.

With both ignition systems, maximum combustion pressures above 2.00 MPa are obtained, reaching 2.54 MPa when steel wire is used as the ignition system. These pressures are much higher than the 0.80 MPa reported in the literature (Cashdollar, 2000), although this study is focused in dust explosions, in 120 dm^3 explosion chambers. On the other hand, the authors have made a comparison between static and dynamic pressure sensors, prior to the tests. The conclusion was that there are differences between the maximum pressures registered by both, which indicated that the use of static pressure sensors limit the study of the explosiveness of methane-air mixtures.

Maximum pressures are reached with methane concentrations between 8.0 and 9.0% with laser and steel wire ignitions, respectively. These values are therefore very similar to the concentration obtained for the calculations associated with ideal conditions.

In this case, it is necessary to point out the occurrence of erratic pressure values, which is mainly due to the difficulty of working with such a small chamber. On the other hand, given that the ignition source has little impact on the maximum value of the pressure reached and that the steel wire is less complex to operate, it was decided that it should be the ignition source for the rest of the tests carried out, both in Chamber 1 and in the rest of the chambers.

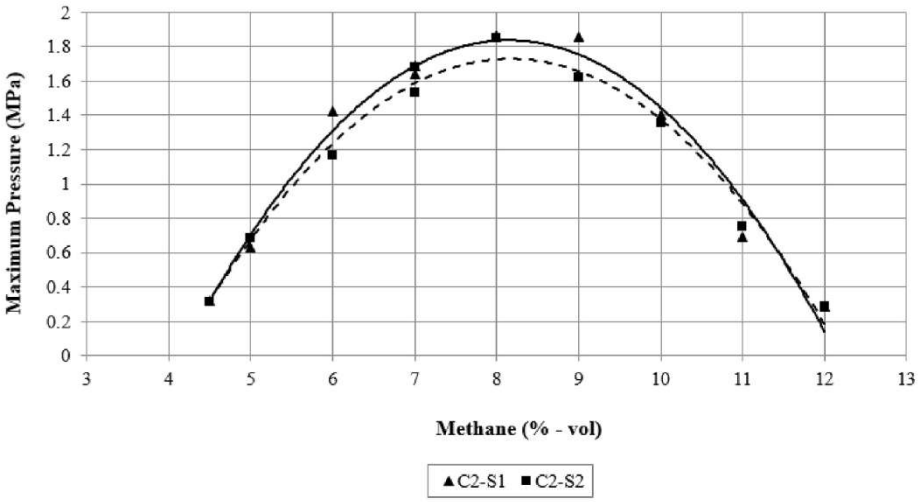

Fig. 9. Maximum pressure reached in wire ignition in Chamber 2.

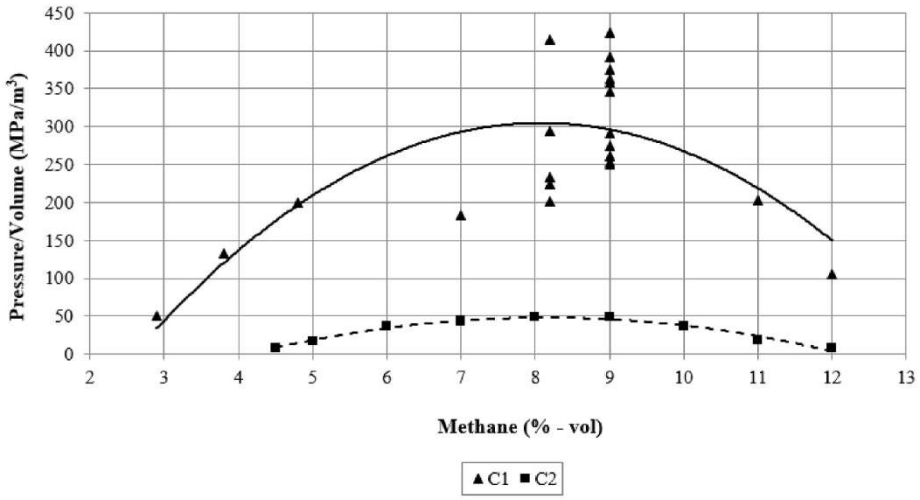

Fig. 10. Comparison, by means of standardised pressure, of explosive chambers.

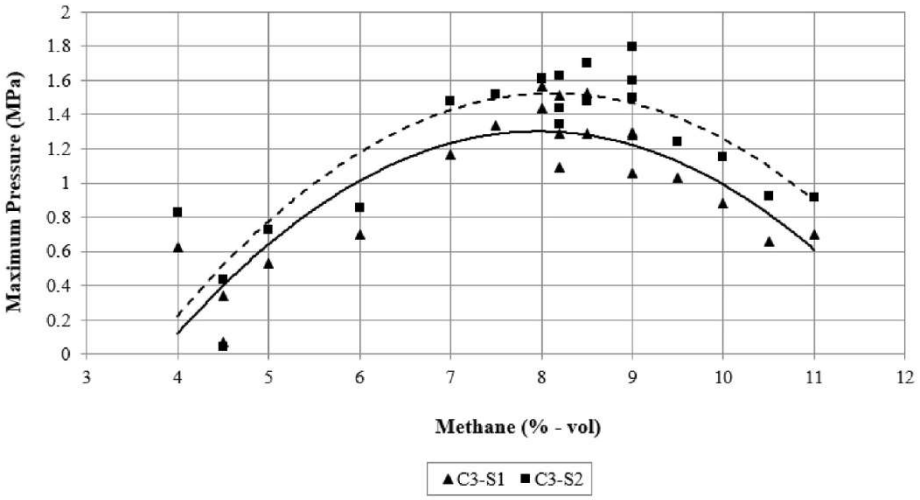

Fig. 11. Maximum pressure reached by wire ignition in Chamber 3.

In Chamber 2, 10 tests were performed that achieved ignition, using steel wire as the ignition source. Methane concentrations between 4.0 and 14.0% were used. Two diametrically distributed sensors, named C2 – S1 and C2 – S2, were used to measure the pressure.

Maximum pressures of 1.80 MPa were recorded at both sensors (Fig. 9), which is lower than in Chamber 1, but with similar concentrations (between 8.0 and 9.0% methane). In addition, ignitions were recorded for methane contents varying between 4.5% and 12.0%. However, the fact that no ignitions were achieved either below or above these values does not indicate that this is the explosion range for Chamber 2, but rather that combustion is not initiated at all times. In other words, the probability of ignition decreases below and above these values.

Fig. 10 shows the effect of the volume of the chamber over the maximum pressure comparing the normalized pressure, that it is to say, the maximum pressure divided by the volume of the chamber. From the figure, it is possible to say that in the chamber 1 the highest normalized pressure is reached. Therefore, at equal methane concentration, the smaller volume chambers are more dangerous due to for a smaller mass of methane introduced into the ignition chamber, the pressures recorded per unit volume are higher.

In Chamber 3, 21 test explosions were achieved employing steel wire as ignition source. The methane concentrations used ranged from 4.0 to 14.0% (Fig. 11). In this chamber, two pressure sensors were used: C3–S1, located in the vicinity of the explosion, and C3–S2, located 80 cm from the previous one.

In terms of maximum pressures, sensor C3 – S1 recorded 1.50 MPa, while sensor C3–S2 recorded 1.80 MPa, for methane concentrations of 8.0 and 9.0%, respectively. Therefore, the highest pressures are collected at the sensor furthest away from the ignition point. This is because the mass fraction burned increases progressively, as pressure and temperature rise. The pressure increase with distance is 0.15 MPa/m, although it appears that the higher the pressure generated by the explosion, the lower this ratio, which drops to 0.13 MPa/m for methane concentrations between 7.5 and 8.0%. This increase in the pressure is in accordance with different published studies about cylindrical chambers (Kundu et al., 2017), (Zhang and Ma, 2015), (Kasmani et al., 2013).

In addition, Fig. 11 shows a large dispersion in pressure values for low methane concentrations, due to a higher difficulty in combustion progress, resulting in erratic pressure values.

A comparison of the results obtained in Chamber 2 and Chamber 3 with the same volume of 38 dm^3, but with a different shape, indicates that the pressure values are higher in the spherical chamber, hence a more unfavourable detonation from a safety point of view. However, the differences are not very significant, and the explosion effects should not be expressed solely as a function of the maximum pressure.

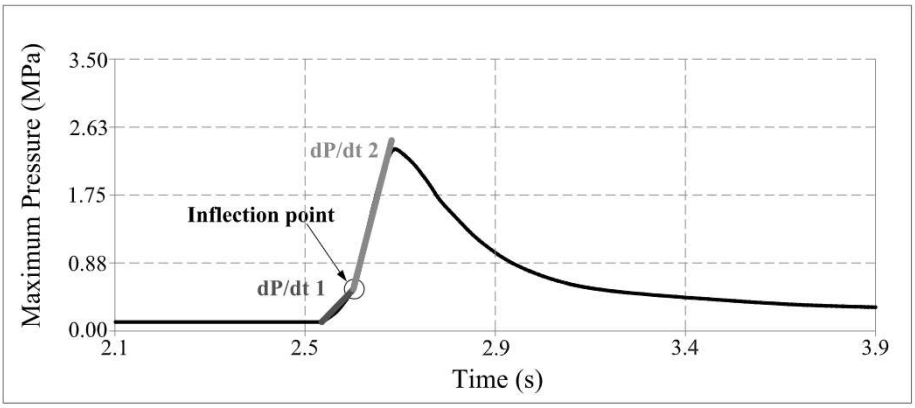

Fig. 12. Rate of pressure in Chamber 1, with steel wire as ignition source and a methane concentration of 8%.

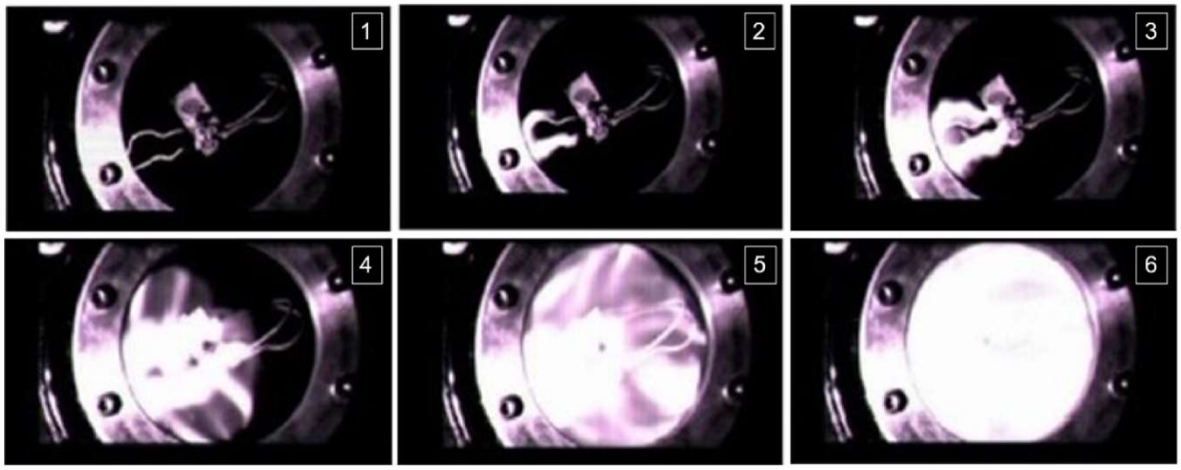

Fig. 13. Example of an explosion propagation sequence in Chamber 1.

3.3. Rate of pressure

The rate of pressure shows the evolution of the pressure over time. Regardless of the chamber used, and with atmospheric pressure as initial pressure, the rate of pressure shows three very distinct zones, as shown in Fig. 12:

- A first pressure rise section referred to as **rate of pressure rise 1** (**dP/dt 1** in Fig. 12).
- A second rising section, called **rate of pressure rise 2** (**dP/dt 2** in Fig. 12), with a greater slope of the curve and where the maximum pressures are reached.
- A third section where temperature and pressure decrease.

The combustion velocity and thus the rate of pressure are functions of the temperature, the initial pressure and the turbulence. Initially, the pressure rise is slower, since the dominant factor is the temperature that increases due to combustion. At the inflection point of the curve, the change in slope is greater, since the temperature increases and, simultaneously, turbulence phenomena associated with the reflections of the pressure waves appears (Fig. 13). Thus, a turbulent front has a larger surface area and, consequently, a higher combustion velocity. The maximum pressure value is recorded at the end of the reaction. From this point and as the exchange of heat between the hot gases and the wall takes place all the time, the pressure and temperature drop to atmospheric values.

In the three chambers, it has been observed that the maximum rate of pressures occur for methane concentrations of around 8.0%, coinciding with the maximum pressure values. However, in Chamber 3, and due to the arrangement of the sensors, a certain time delay is observed in the pressure data recorded by sensor C3–S2 compared to sensor C3–S1, producing the change in gradient. This delay is minimal for methane concentrations of around 8.0–9.0%, where the maximum pressures occur, and increases for the rest of the concentrations, indicating a lower velocity of the pressure wave (Fig. 14).

3.4. Acceleration wave

In explosions is very important identify detonation versus deflagration since the effect in the surrounding is very different. In a detonation, the wavefront goes ahead of maximum pressure with values over 1 MPa and supersonic velocities of propagation, while in a deflagration the pressure is smaller and the velocity of propagations is subsonic (Lees, 2012).

There are numerous studies that not only identify the two explosion phases but also the transition from deflagration to detonation. In most of them, parameters as maximum pressure, velocity of propagation or flame acceleration are employed as identifiers of the process (Kagan and Sivashinsky, 2017), (Oran and Gamezo, 2007), (Gamezo et al., 2008).

In this paper, the accelerometers measure the effect of the explosion over the chamber and not the flame acceleration. This is an initial study, but the comparison between the maximum pressure and the acceleration of the chamber seems identify the detonation versus deflagration, being:

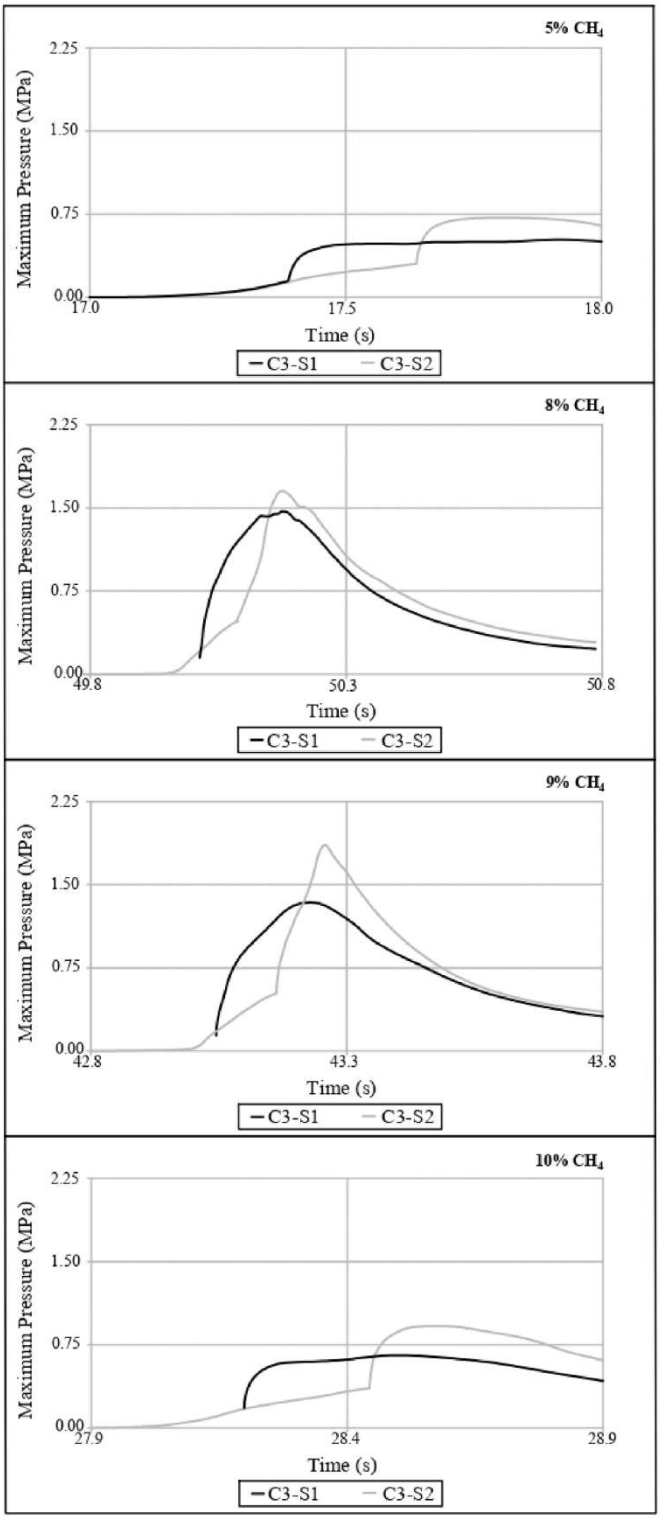

Fig. 14. Pressure evolution in Chamber 3, for different methane concentrations.

- Deflagration where maximum pressures don't happen at the same time that the maximum acceleration of the chamber and the amplitude of this one is smaller than 2.5 m/s^2 (Fig. 15).
- Detonation where maximum pressures happen at the same time that maximum acceleration of the chamber with values over 150 m/s^2 and even 500 m/s^2 (Fig. 16).

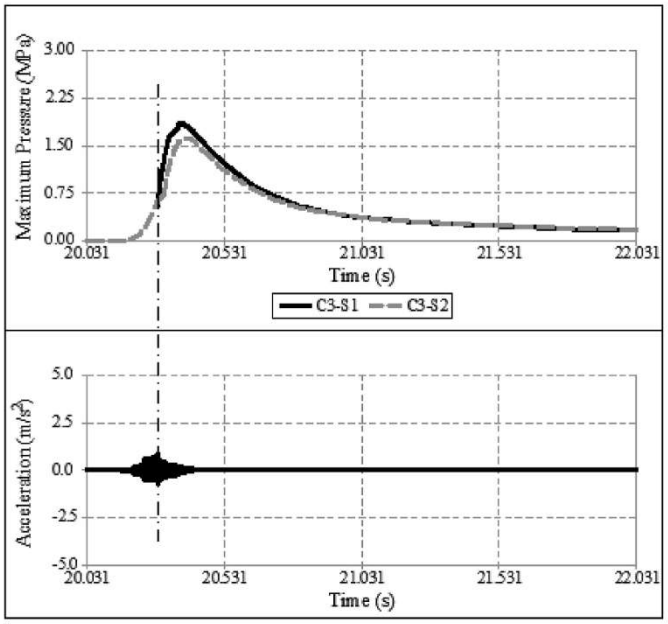

Fig. 15. Relationship between pressures and accelerations in Chamber 2, for a methane concentration of 9%.

Following the difference indicated, a comparison of the maximum pressures recorded in Chambers 2 and 3 shows that, a priori, detonations in spherical chambers are more unfavourable than in tubular chambers. Although, the pressures are not very different from each other. On the other hand, when self-ignition occurs, in the tubular chamber it is more frequent the detonation while in the spherical chamber is the deflagration. Moreover, in the tubular chamber, the accelerations are higher than in the spherical chamber. Therefore, considering the accelerations as an indicator of the transmitted forces, it can be stated that the tubular geometry is much more unfavourable, in terms of safety, than the spherical chambers.

4. Conclusions

In this paper, the explosion phenomenon of methane - air mixtures is analysed by means of tests carried out in three different explosion chambers (two quasi-spherical and one cylindrical), sealed and prepared to withstand high pressures. From the tests carried out, it is concluded that:

- The sizes of the flakes used to initiate ignition influence the minimum energy required to achieve ignition. Thus, the larger the flake, the more energy must be applied to reach the temperature required to initiate ignition. Therefore, small flakes, which are mostly present in mechanical starting processes, are the most problematic as they require less energy to reach the ignition temperature.
- The critical energy required to produce the explosion increases with the concentration of methane inside the explosive limits.
- Methane concentrations between 8 and 9% lead to maximum pressures above 1.50 MPa and even up to 2.50 MPa, which is much higher than the maximum values reported in the literature of around 0.80 MPa (Cashdollar, 2000).
- The explosion range is estimated from the pressure-methane concentration graphs, yielding ignition values with a methane concentration of 2.9%, which is well below what is expected. However, in this case it should rather be treated as the limits where there is a higher probability of ignition, as it would be necessary to carry out a larger number of tests to determine the actual limits.

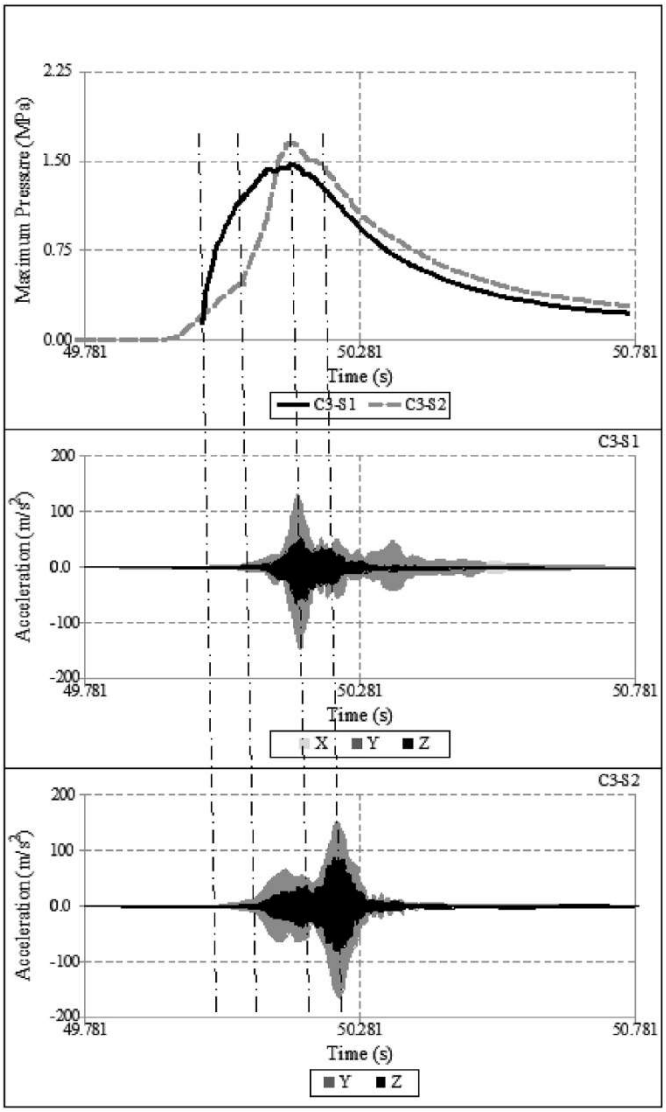

Fig. 16. Relationship between pressures and accelerations in Chamber 3, for a methane concentration of 8%.

- The volume of the chamber does not significantly influence the maximum explosion pressure. However, in larger chambers the pressure per unit volume is lower in larger chambers. In other words, at the same methane concentration, smaller volume chambers are more dangerous.
- The shape of the chamber slightly influences the maximum explosion pressure, increasing its value in spherical versus tubular chambers.
- The pressure increases away from the point of ignition, being the pressure increase with distance of 0.15 MPa/m, although the higher the pressure generated by the explosion, the lower this ratio is. This fact is very relevant for very long lengths, such as a mine shaft or tunnel.
- The evolution of pressure shows initially a slow increment due to the increase of the temperature. After that, the increase of the pressure is faster because turbulence phenomena associated with pressure wave reflections come into play.
- The time of the test at which the maximum acceleration occurs determines whether deflagration or detonation occurs. In the quasi-spherical chambers, deflagrations mainly occur, whereas in the tubular chamber, detonations occur. This reinforces the fact that the tubular geometry is more dangerous, even though the maximum pressures reached in both types of chambers are similar.

Author contribution

Martina-Inmaculada Álvarez-Fernández: Methodology; Conceptualization; Writing—review and editing; Supervision. **María-Belén Prendes-Gero**: Formal analysis; Lab tests; Writing—original draft preparation; Writing—review and editing. **Isaac Pola-Alonso**: Methodology; Formal analysis; Lab tests. **Lucía Conde-Fernández**: Formal analysis; Lab tests; Writing—original draft preparation; Writing—review and editing. **Juan-Carlos Luengo-García**: Conceptualization; Methodology; Supervision.

Declaration of competing interest

The authors declare that they have no known competing financial interests or personal relationships that could have appeared to influence the work reported in this paper.

Data availability

The data that has been used is confidential.

References

Ajrash, M.J., Zanganeh, J., Moghtaderi, B., 2016a. Effects of ignition energy on fire and explosion characteristics of dilute hybrid fuel in ventilation air methane. J. Loss Prev. Process. Ind. 40, 207–216. https://doi.org/10.1016/j.jlp.2015.12.014.

Ajrash, M.J., Zanganeh, J., Moghtaderi, B., 2016b. Methane-coal dust hybrid fuel explosion properties in a large scale cylindrical explosion chamber. J. Loss Prev. Process. Ind. 40, 317–328. https://doi.org/10.1016/j.jlp.2016.01.009.

Beduneau, J.-L., Bonggyu, K., Zimmer, L., Ikeda, Y., 2003. Measurements of minimum ignition energy in premixed laminar methane/air flow by using laser induced spark. Combust. Flame 132 (4), 653–665. https://doi.org/10.1016/S0010-2180(02)00536-9.

Cashdollar, K.L., 1996. Coal dust explosibility. J. Loss Prev. Process. Ind. 9, 65–76. https://doi.org/10.1016/0950-4230(95)00050-X, 1 SPEC. ISS.

Cashdollar, K.L., 2000. Overview of dust explosibility characteristics. J. Loss Prev. Process. Ind. 13 (3–5), 183–199. https://doi.org/10.1016/S0950-4230(99)00039-X.

Dhillon, B.S., 2010. Mine Safety: A Modern Approach, first ed. Springer. https://doi.org/10.1007/978-1-84996-115-8.

Gamezo, V.N., Ogawa, T., Oran, E.S., 2008. Flame acceleration and DDT in channels with obstacles: effect of obstacle spacing. Combust. Flame 155 (1–2), 302–315. https://doi.org/10.1016/j.combustflame.2008.06.004.

Gharagheizi, F., 2008. Quantitative structure-property relationship for prediction of the lower flammability limit of pure compounds. Energy Fuel. 22 (5), 3037–3039. https://doi.org/10.1021/ef800375b.

Going, J.E., Chatrathi, K., Cashdollar, K.L., 2000. Flammability limit measurements for dusts in 20-L and 1-m3 vessels. J. Loss Prev. Process. Ind. 13 (3–5), 209–219. https://doi.org/10.1016/S0950-4230(99)00043-1.

Johansen, C.T., Ciccarelli, G., 2009. Visualization of the unburned gas flow field ahead of an accelerating flame in an obstructed square channel. Combust. Flame 156 (2), 405–416. https://doi.org/10.1016/j.combustflame.2008.07.010.

Kagan, L., Sivashinsky, G., 2017. Parametric transition from deflagration to detonation: runaway of fast flames. Proc. Combust. Inst. 36 (2), 2709–2715. https://doi.org/10.1016/j.proci.2016.09.026.

Kasmani, R.M., Andrews, G.E., Phylaktou, H.N., 2013. Experimental study on vented gas explosion in a cylindrical vessel with a vent duct. Process Saf. Environ. Protect. 91 (4), 245–252. https://doi.org/10.1016/j.psep.2012.05.006.

Kindracki, J., Kobiera, A., Rarata, G., Wolanski, P., 2007. Influence of ignition position and obstacles on explosion development in methane-air mixture in closed vessels. J. Loss Prev. Process. Ind. 20 (4–6), 551–561. https://doi.org/10.1016/j.jlp.2007.05.010.

Kundu, S., Zanganeh, J., Moghtaderi, B., 2016. A review on understanding explosions from methane-air mixture. J. Loss Prev. Process. Ind. 40, 507–523. https://doi.org/10.1016/j.jlp.2016.02.004.

Kundu, S., Zanganeh, J., Eschebach, D., Mahinpey, N., Moghtaderi, B., 2017. Explosion characteristics of methane–air mixturesin a spherical vessel connected with a duct. Process Saf. Environ. Protect. 111, 85–93. https://doi.org/10.1016/j.psep.2017.06.014.

Lees, F.P., 2012. Lees' loss prevention in the process industries. In: Hazard Identification, Assessment and Control, fourth ed. Sam Mannan, UK. https://doi.org/10.1016/C2009-0-24104-3.

Li, J., Wang, X., Guo, J., Zhang, J., Zhang, S., 2020. Effect of concentration and ignition position on vented methane–air explosions. J. Loss Prev. Process. Ind. 68 (October), 104334 https://doi.org/10.1016/j.jlp.2020.104334.

Li, P., Huang, P., Liu, Z., Du, B., Li, M., 2019. Experimental study on vented explosion overpressure of methane/air mixtures in manhole. J. Hazard Mater. 374 (September 2020), 349–355. https://doi.org/10.1016/j.jhazmat.2019.04.046.

Ma, C., Wang, Z.R., Cui, Y.Y., Ma, W.D., 2018. Effect of ignition position on methane explosion in spherical vessel with a pipe. Procedia Eng. 211, 538–545. https://doi.org/10.1016/j.proeng.2017.12.046.

Mynarz, M., Lepík, P., Serafin, J., 2012. Experimental determination of deflagration explosion characteristics of methane-air mixture and their verification by advanced numerical simulation. WIT Trans. Built Environ. 126, 169–178. https://doi.org/10.2495/SU120151.

Oran, E.S., Gamezo, V.N., 2007. Origins of the deflagration-to-detonation transition in gas-phase combustion. Combust. Flame 148 (1–2), 4–47. https://doi.org/10.1016/j.combustflame.2006.07.010.

Phuoc, T.X., White, F., 1999. Laser-induced spark ignition of CH4-air mixtures. Combust. Flame 119, 203–216. https://doi.org/10.1016/S0010-2180(99)00051-6.

Radford, J., 2014. What Happened Tragic Day of Mt Kembla Mine Disaster. http://www.illawarramercury.com.au/story/2441786/whathappened-tragic-day-of-mt-kembla-mine-disaster/.

Rivas, B., 2016. De Havilland Comet Manual: Insights into the Design, Construction and Operati (Owners' Workshop Manual). Haynes Publishing UK.

Rocourt, X., Awamat, S., Sochet, I., Jallais, S., 2014. Vented hydrogen-air deflagration in a small enclosed volume. Int. J. Hydrogen Energy 39 (35), 20462–20466. https://doi.org/10.1016/j.ijhydene.2014.03.233.

Solberg, D.M., Pappas, J.A., Skramstad, E., 1981. Observations of flame instabilities in large scale vented gas explosions. Symposium (International) on Combustion 18 (1), 1607–1614. https://doi.org/10.1016/S0082-0784(81)80164-6.

Taveau, J.R., Lemkowitz, S.M., Hochgreb, S., Roekaerts, D.J.E.M., 2019. Metal dusts explosion hazards and protection. Chem. Eng. Transact. 77, 7–12. https://doi.org/10.3303/CET1977002.

Xu, Y., Huang, Y., Ma, G., 2020. A review on effects of different factors on gas explosions in underground structures. Undergr. Space 5 (4), 298–314. https://doi.org/10.1016/j.undsp.2019.05.002.

Yang, H.N., Chen, J.H., Chiu, H.J., Kao, T.J., Tsai, H.Y., Chen, J.R., 2016. Confined vapor explosion in Kaohsiung City - a detailed analysis of the tragedy in the harbor city. J. Loss Prev. Process. Ind. 41, 107–120. https://doi.org/10.1016/j.jlp.2016.03.017.

Zhang, Q., Ma, Q.J., 2015. Dynamic pressure induced by a methane–air explosion in a coal mine. Process Saf. Environ. Protect. 93, 233–239. https://doi.org/10.1016/j.psep.2014.05.005.